Progress In Electromagnetics Research C, Vol. 70, 63–72, 2016

Design of a Microstrip Filtering Balun with a Wide Stopband

Jun-Mei Yan[1, *], Liang-Zu Cao[1, 2], and Hai-Ying Zhou[1]

Abstract—A microstrip filtering balun with a wide stopband is presented. Its filtering function is realized by four meandering stepped impedance resonators (SIRs). Except for an identical fundamental-mode resonant frequency, the SIRs have different high-order resonant frequencies. Thus, the parasitic passbands are suppressed, and a wide stopband is achieved. The unbalance-to-balance transition is accomplished by introducing two coupling output ports at two symmetry positions of the output SIR. The voltages at symmetrical positions have equal magnitudes and opposite phases, thus, signals coupled from the symmetrical positions also have equal magnitudes and opposite phases, i.e., balanced output signals are achieved. A more general design approach is discussed in detail, and the proposed approach is similar to the design method of the conventional filter except that a small modification is made. Additionally, two kinds of external coupling structures, microstrip coupling lines and tapped line, are compared in terms of stopband performance. The comparison shows that better stopband performance is observed when utilizing the microstrip coupling lines as the external coupling structure. A filtering balun with central frequency of 2.4 GHz and Chebyshev frequency response is designed, fabricated and measured. The measured results give a reasonable agreement with the simulated ones, which verifies the effectiveness of the filtering balun.

1. INTRODUCTION

For a better stability, more and more circuits, both high-speed digital ones and analog microwave ones, adopt differential circuits due to their strong immunity to environmental noises. Thus, the need for balun is increasing. Balun accomplishes the transition from unbalanced circuits to balanced ones [1–4]. Recently, to miniaturize circuit size, many researchers try to integrate filtering function into balun devices, thus, more novel baluns with filtering function are proposed. They are called filtering balun.

In [5–9], filtering function is accomplished by a loop resonator using its two degenerate modes. Two positions with out-of-phase signals at the loop resonator are chosen for external coupling, thus, two output ports with balanced signals can be obtained. The open/shorted microstrip parallel coupling lines and stepped impedance microstrip line are introduced to the loop resonator, and a wideband filtering balun is realized [5]. By loading a quasi-T shaped open stub on the loop resonator, one more transmission zero above the passband is generated to get a better upper stopband performance [7]. In [8], in each port of the filtering balun, the low-pass unit cells of quarter-wavelength electrical length are inserted to suppress the second- to fourth-order harmonics, and a wider upper stopband is obtained. The loop resonator is loaded with distribution capacitance [9], which not only realizes the size reduction, but also suppresses the spurious response. The filtering balun proposed in [10] has a similar operational mechanism to above loop resonator structure except that a dual-mode cross-slotted patch resonator is used. These filtering balun structures have a common disadvantage, i.e., the higher-than-second-order filtering function is very difficult to be realized, and the design freedom degree of in-band performance is limited.

Received 30 September 2016, Accepted 24 November 2016, Scheduled 12 December 2016

* Corresponding author: Jun-Mei Yan (yjmzhy@163.com).

[1] School of Mechanical and Electronic Engineering, Jingdezhen Ceramic Institute, China. [2] School of Electronic and Optical Engineering, Nanjing University of Science and Technology, China.

A middle metal layer, used as the common ground of the output ports, is inserted into the substrate integrated waveguide (SIW) to realize the equal-magnitude and out-of-phase power division [11], i.e., to get balanced output signals. Then, in each output signal path, four inductive posts are embedded to develop filtering function. In [12], the common ground is inserted into the parallel double-sided microstrip lines instead of SIW in [11] to realize the balanced signal output. Furthermore, in each signal path, a dual-band filtering function is designed. An SIW is also used in [13], and the equal-magnitude and out-of-phase signal outputs are realized by oppositely using the top and bottom metal layers as the ground and signal strip line at two output ports. Furthermore, multiple slots are etched on the top and bottom layers to improve the isolation performance. These multiple-layer structures have an improved performance but are also complicated.

Additionally, many filtering baluns come from differential bandpass filters [14–20]. By keeping one input port of the differential bandpass filter open, the remaining three ports form the filtering balun with the remaining input port as the unbalanced input port and the remaining two output ports as the balanced output ports. The SIRs are designed to have different high-order resonant frequencies in [15], which helps to suppress the spurious responses. In [18], a filtering balun with improved in-band balance performance is proposed by inserting open-circuit coupling lines at the unbalanced input port, and the bandwidth can be controlled by adjusting the characteristic impedance of the microstrip lines. Filtering baluns are extended into having dual-band filtering function [16, 17, 19, 20]. The design method of these filtering baluns modified from the differential bandpass filter is to put the constraint conditions presented in [14] into the design of the differential bandpass filter.

This paper gives a simple fourth-order filtering balun with wide stopband, which is from the differential bandpass filter structure in [21]. As illustrated in [21], magnetic coupling instead of electrical coupling is used to reject high-order harmonics. Additionally, SIRs are used as resonators, which are also designed to have different high-order resonant frequencies, just as [22]. The parasitic passbands are further suppressed, and a wide stopband is achieved. Instead of the design method in [14–19], a more general design method is proposed. Firstly, the desired coupling coefficients and external quality factors are obtained according to the target filtering performance. Then, the desired output quality factor is doubled when it is implemented by a single output port. After that, at the symmetrical position, a identical output port is added, and the output resonator has the same external quality factor as the desired one. The added output port does not change the filtering performance.

The remainder of this paper is organized as follows. In Section 2, the design procedure for the proposed filtering balun with Chebyshev response is discussed in detail, including characterizing the SIRs in terms of the relationship of their resonant frequencies with the physical dimensions, synthesizing the coupling coefficients and the external quality factors according to the target filtering performance and extracting the coupling coefficients and external quality factors. In Section 3, two types of external coupling structures, microstrip coupling lines and tapped line, are compared in terms of the stopband performance. The comparison shows that utilizing the microstrip coupling lines as the external coupling structure has a better stopband performance. In Section 4, for a experimental confirmation, a fourth-order filtering balun is designed, fabricated and measured, and the simulated and measured results are compared. The conclusion is given in Section 5.

2. DESIGN PROCEDURE

2.1. Characterizing SIRs

The schematic layout of a symmetric SIR is shown in Fig. 1(a). The SIR is constructed by microstrip lines with different characteristic impedance and electric length. The dashed line is its symmetry axis. Its resonant frequencies can be controlled by adjusting the ratios of the characteristic impedance Z_1, Z_2 and electric lengths θ_1, θ_2. The input impedance seen from the dashed line to the end is as follows,

$$Z_{in} = jZ_1 \frac{R_z \tan(R_\theta \theta_2) \tan\theta_2 - 1}{R_z \tan\theta_2 + \tan(R_\theta \theta_2)}, \tag{1}$$

where $R_z = Z_1/Z_2$ and $R_\theta = \theta_1/\theta_2$. Both $Z_{in} = 0$ and $Z_{in} = \infty$ indicate occurrence of the resonance. $Z_{in} = 0$ and $Z_{in} = \infty$ are corresponding to the odd-mode and even-mode resonances, respectively. Fig. 1(b) shows a diagram of the first four high-order resonant frequencies normalized to the fundamental

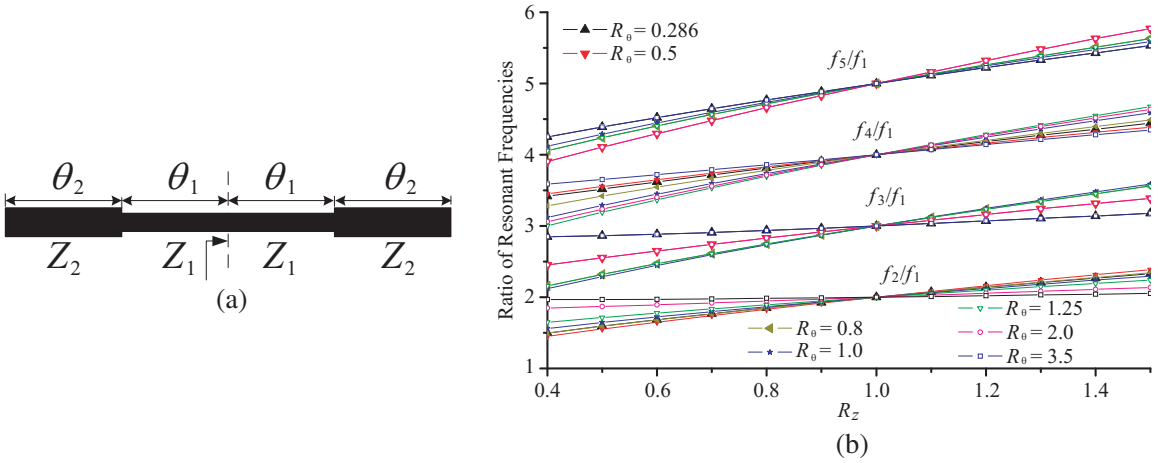

Figure 1. (a) The schematic layout of a symmetric SIR and (b) its normalized high-order resonant frequencies against various R_Z and R_θ.

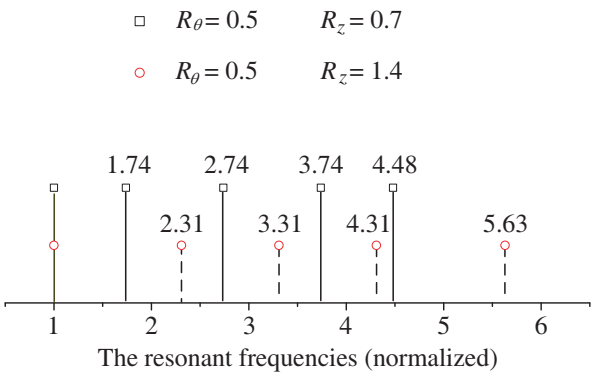

Figure 2. Distribution of the normalized resonant frequencies for $R_\theta = 0.5$, $R_z = 0.7$ and $R_\theta = 0.5$, $R_z = 1.4$.

resonant frequency against various R_z and R_θ. As shown in Fig. 1(b), for each high-order resonance, when R_z changes, the normalized resonant frequencies change approximately linearly. The value of R_θ determines the variation range. Thus, by choosing proper values of R_z and R_θ, the different SIRs in a single filter can be designed to have different high-order frequencies but keep the fundamental resonant frequency equal. As an example, Fig. 2 gives a distribution of the normalized resonant frequencies when $R_\theta = 0.5$, $R_z = 0.7$ and $R_\theta = 0.5$, $R_z = 1.4$. Obviously, by this approach, the spurious passband will be suppressed, and a wide stopband can be achieved.

Two SIRs corresponding to $R_\theta = 0.5$, $R_z = 0.7$ (Type A) and $R_\theta = 0.5$, $R_z = 1.4$ (Type B) are designed, and their fundamental resonant frequency is 2.4 GHz. The geometry is shown in Fig. 3(a). A substrate with thickness of 0.8 mm and relative dielectric constant of 2.55 is used. The low-impedance microstrip line has a width of 1.5 mm, whose characteristic impedance is 64.1 Ω, and the high-impedance microstrip line has a width of 0.8 mm, whose characteristic impedance is 90.8 Ω. Using HFSS 15.0 as the full-wave simulation tool, the first five resonant frequencies of two SIRs are found as listed in Fig. 3(b). It is very close to the results in Fig. 2.

2.2. Synthesis of the Coupling Coefficients and External Quality Factors

For the bandpass filter with Chebyshev frequency response, its coupling coefficients and external quality factors can be derived from the element values of its corresponding low-pass prototype filter using

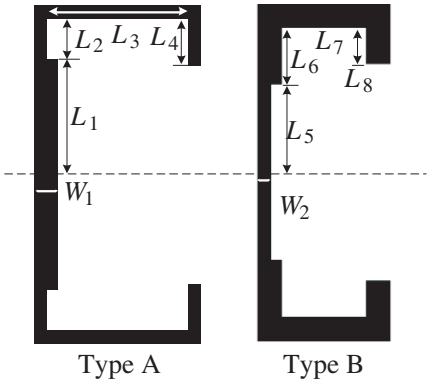

(a)

Resonant (GHz) Frequency	f_1	f_2	f_3	f_4	f_5
		f_2/f_1	f_3/f_1	f_4/f_1	f_5/f_1
Type A	2.394	4.253	6.501	8.828	10.947
		1.78	2.71	3.69	4.57
Type B	2.391	5.719	7.844	10.181	13.47
		2.39	3.28	4.26	5.63

(b)

Figure 3. (a) Geometry, $W_1 = 1.5, W_1 = 0.8, L_1 = 7.5, L_2 = 2.5, L_3 = 9.5, L_4 = 3.0, L_5 = 5.7, L_6 = 3.6, L_7 = 5.5, L_8 = 2.3$, (all are in mm). (b) Resonant frequencies from full-wave simulation.

following equations,

$$M_{i,i+1} = \frac{FBW}{\sqrt{g_i g_{i+1}}} \quad \text{for} \quad i = 1, \ldots, n-1, \tag{2}$$

$$Q_{e1} = \frac{g_0 g_1}{FBW}, \quad Q_{en} = \frac{g_n g_{n+1}}{FBW}, \tag{3}$$

where n is the filter's order number, $g_i\,(i = 0, \ldots, n+1)$ the element values of the low-pass prototype filter, and FBW the fractional bandwidth. For example, for the fourth-order bandpass filter with insertion loss of 0.01 dB and FBW = 4%, its low-pass prototype element values are $g_0 = 1.0$, $g_1 = 0.7128$, $g_2 = 1.2003$, $g_3 = 1.3212$, $g_4 = 0.6476$, $g_5 = 1.1007$. According to Eq. (2), the coupling coefficients are $M_{12} = M_{34} = 0.0432$ and $M_{23} = 0.0318$. According to Eq. (3), the external quality factors are $Q_{e1} = Q_{e4} = 17.8$.

Because the filter is designed for having balun function, the output resonator should have two identical coupling output ports. Thus, the external quality factor of the output resonator with a single coupling output port should be 36.4, which can be obtained from the following formula,

$$\frac{1}{Q_{e4}} = \frac{1}{Q'_{e4}} + \frac{1}{Q'_{e4}}, \tag{4}$$

where Q_{e4} is the total external quality factor of the output resonator and Q'_{e4} the external quality factor of the output resonator with only one coupling output port. Fig. 4(a) gives a coupling scheme showing the transformation from the filter to the filtering balun. Using the formulas presented in [23], the ideal S parameters of the filter and filtering balun can be obtained and shown in Fig. 4(b). It can be observed that after the two identical ports are coupled to the output resonator, the reflection coefficients are not fully affected. The signal is divided into two ways with equal magnitude. The out-of-phase coupling positions at the output resonator are chosen to realize the out-of-phase output signals, which will be discussed in Section 3.

2.3. Extraction of Coupling Coefficients and External Quality Factors

Both coupling coefficients and quality factors can be extracted using the method described in [24, Chapter 8]. The formulas are as follows

$$Q_e = \frac{\omega_0 \tau}{4}, \tag{5}$$

$$M = \frac{f_{p1}^2 - f_{p2}^2}{f_{p1}^2 + f_{p2}^2}, \tag{6}$$

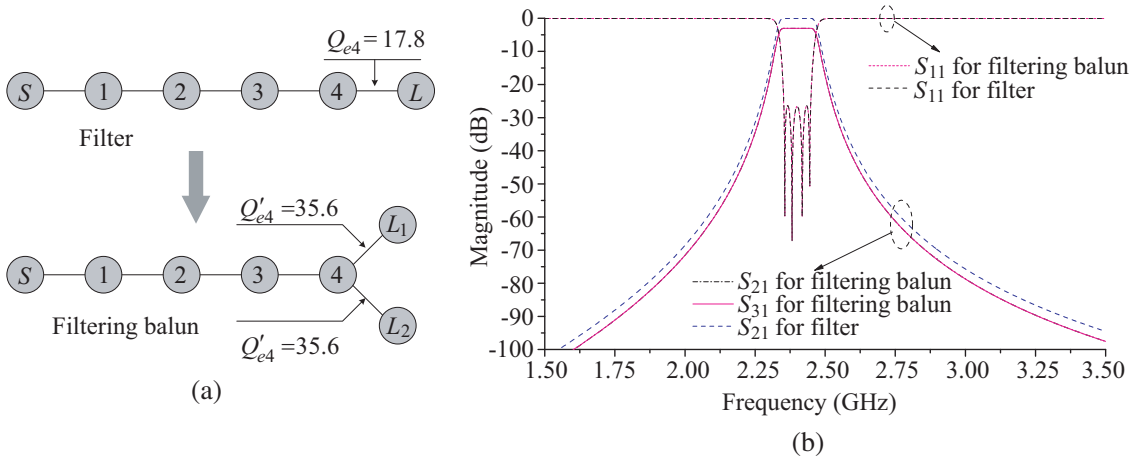

Figure 4. (a) The coupling scheme and (b) their ideal S parameters of the fourth-order filter and its corresponding balun.

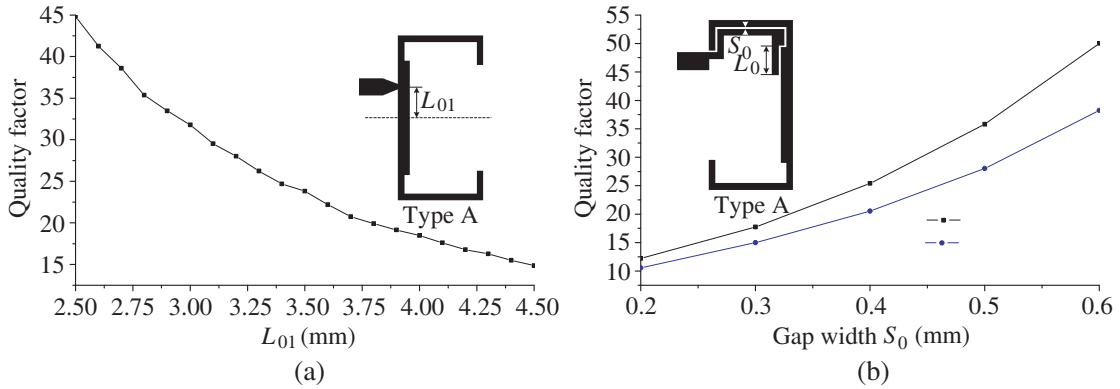

Figure 5. The extracted quality factors of the Type A SIR and the corresponding extraction model (a) with tapped line as external coupling structure against various tapped points L_{01} and (b) with coupling lines as external coupling structure against various gap widths S_0 and lengths L_0.

where ω_0 is the resonant frequency, τ the group delay at the resonant frequency, and f_{p1}, f_{p2} are the resonance frequencies at weak coupling. Fig. 5 shows the extracted external quality factors of type A resonator with two external coupling styles, i.e., tapped lines and coupling line. Fig. 5(a) indicates that a longer distance from the symmetric line to the feeding point means a stronger external coupling. A narrower gap of the coupling lines means a stronger coupling, which is confirmed by Fig. 5(b). Fig. 6 shows the extracted coupling coefficients against various gap widths for different resonators and coupling styles.

3. DESIGN RESULTS AND PERFORMANCE COMPARISON OF TWO FILTERING BALUNS

A symmetric fourth-order filter and its corresponding filtering balun are designed. The geometry is shown in Fig. 7 (Filter I and Balun I). The tapped line is used as the external coupling structure. The filter is targeted to have the central frequency of 2.4 GHz, insertion loss of 0.01 dB and fractional bandwidth of 4%. The quality factors and coupling coefficients are calculated in Section 2.2. According to Figs. 5 and 6, $L_{01} = 4.1$ mm, $L_{02} = 2.8$ mm, $S_1 = 2.7$ mm, $S_2 = 0.7$ mm. The simulated S parameters of the filter are shown in Fig. 8(a). There is a spurious response at 5.7 GHz, and the insertion loss is 12.4 dB, which is corresponding to the second resonant frequency of type B resonator. Other high-order

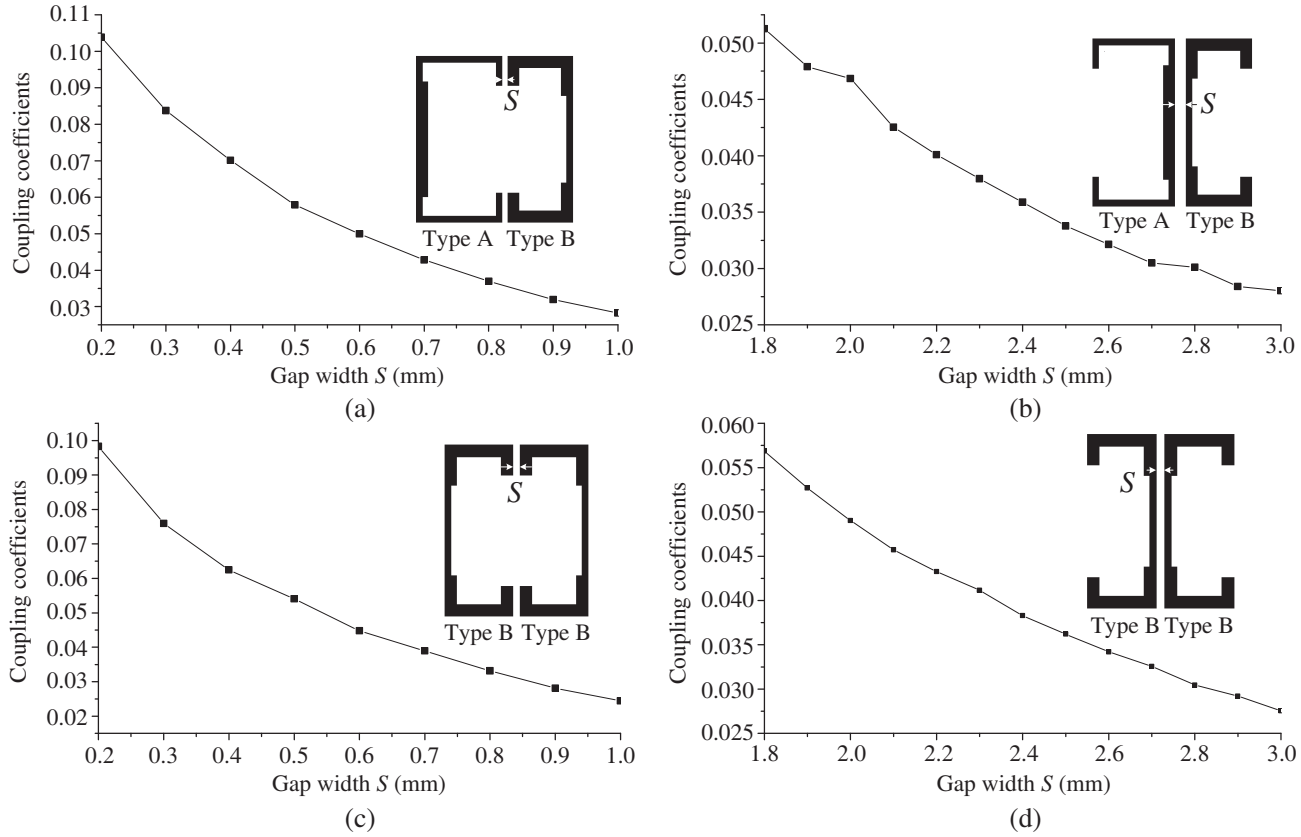

Figure 6. The extracted coupling coefficients and the extraction model. (a) The electric coupling between Type A and B SIRs against various gap widths S. (b) The magnetic coupling between Type A and B SIRs against various gap widths S. (c) The electric coupling between two Type B SIRs against various gap widths S. (d) The magnetic coupling between two Type B SIRs against various gap widths S.

spurious responses are also marked. The spurious responses degrade the stopband performance. Based on the filter, a filtering balun is designed, whose layout is also shown in Fig. 7. The tapped points of the output ports are symmetrically located at the output resonator. The fundamental resonant mode of the SIR is odd mode, and the symmetric tapped points have out-of-phase voltages, thus, the two output ports have out-of-phase output signals. The simulated phase difference of the two output ports is shown in Fig. 8(b), which is in agreement with the predicted one. Additionally, according to Eq. (4), Q'_{e4} is two times of Q_{e4}, which is the cause that L_{02} is not equal to L_{01}. The simulated S-parameters of the filtering balun are also given in Fig. 8(a) and in agreement with the predicted. But filter I and balun I have a degraded stopband performance due to the second spurious resonance of type B resonator.

Another similar filter and the corresponding filtering balun with improved stopband performance are also designed, which have coupling line as the external coupling structure. The layouts are shown in Fig. 9 (Filter II and Balun II). The design is based on the same quality factors and coupling coefficients as Filter I and Balun I. Fig. 10 gives the simulated S parameters and the phase difference of the output ports. Compared with Filter I, the stopband performance is obviously improved. The improvement is obviously caused by the different external coupling style. The tapped line structure has a stronger signal transmission at non-resonance frequency due to its electric contact with the resonator, just as Filter I does. While filter II has coupling line as the external coupling structure, which has no electric contact with the resonator, and the transmission signal is weaker at non-resonance frequency. Thus, the spurious responses are greatly suppressed.

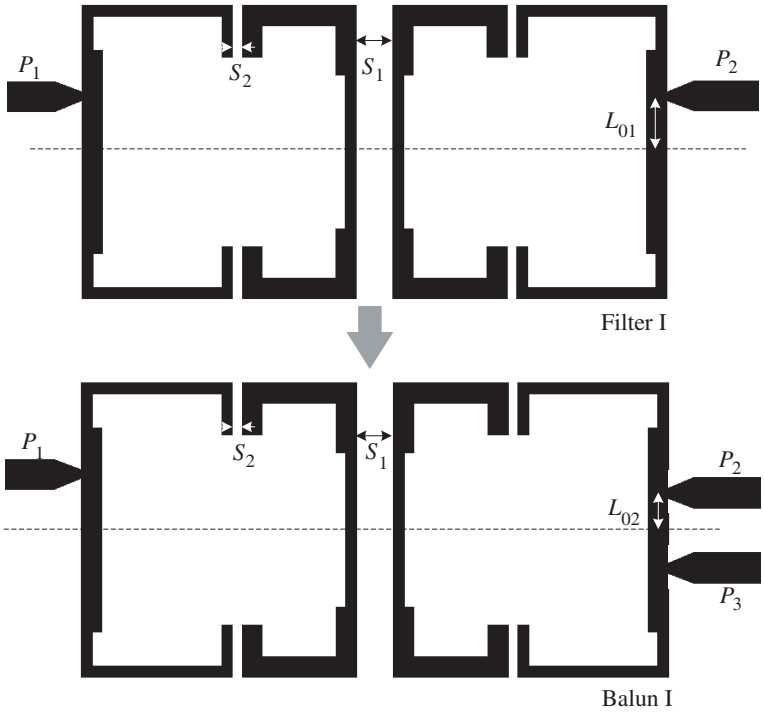

Figure 7. Geometry of the fourth-order bandpass filter (Filter I) and its corresponding filtering balun (balun I).

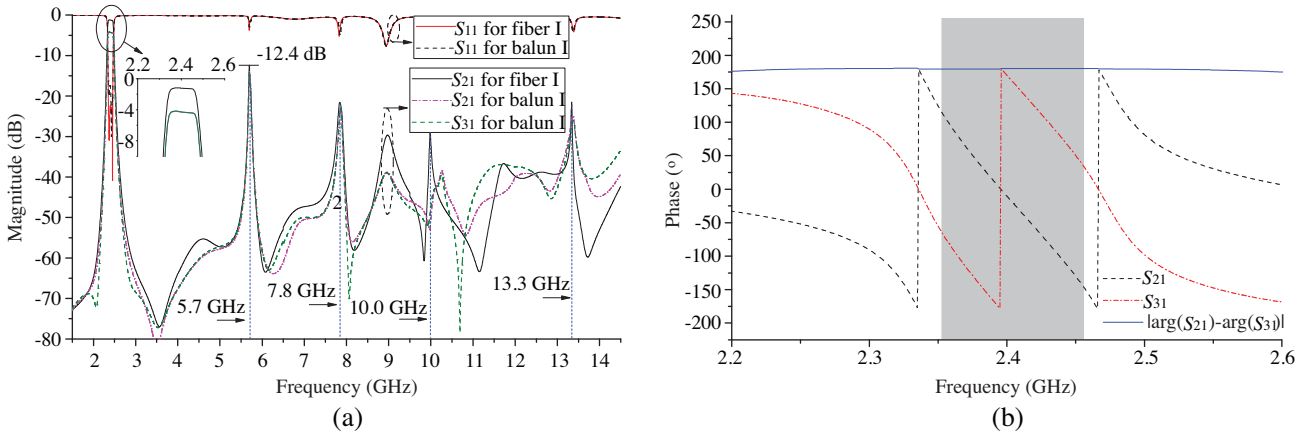

Figure 8. The simulated (a) S parameters, (b) phase and phase difference of the two output ports of the fourth-order filter and its corresponding filtering balun. (Filter I and balun I).

4. EXPERIMENTAL CONFIRMATION

For demonstration, filtering balun II is fabricated and measured. The vector network analyzer (Agilent E5071B) is used for measurement. A photograph and its physical dimensions are given in Fig. 11. The simulated and measured S parameters are shown in Fig. 12(a). The measured central frequency of the passband is at 2.4 GHz. The measured return loss is above 7.5 dB, and the corresponding bandwidth is 3.5%. The measured insertion loss of the two output ports are about 7.4 dB with a unbalance level of 0.3 dB. A spurious response with insertion loss of 34 dB exists at 4.4 GHz. Up to the measurement upper-limit frequency of 8.5 GHz, the insertion loss is less than 30 dB. The simulated and measured phase differences of the two output ports are shown in Fig. 12(b). A measured phase unbalance level

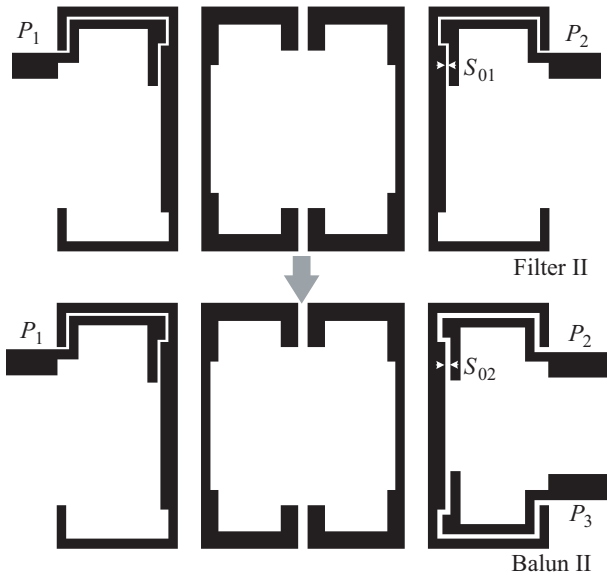

Figure 9. Geometry of the fourth-order bandpass filter (Filter II) and its corresponding filtering balun (balun II).

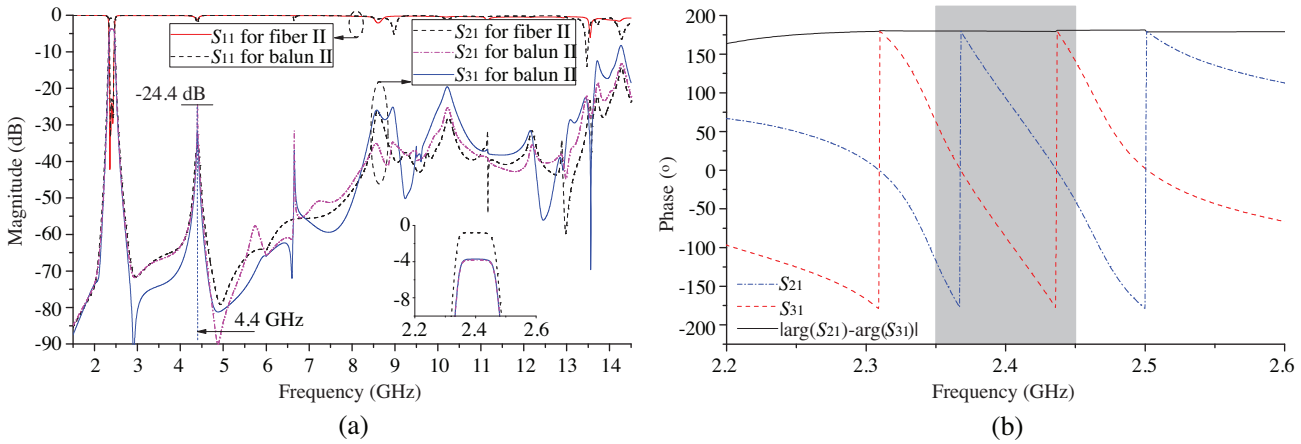

Figure 10. The simulated (a) S parameters, (b) phase and phase difference of the two output ports of the fourth-order filter and its corresponding filtering balun. (Filter II and balun II)

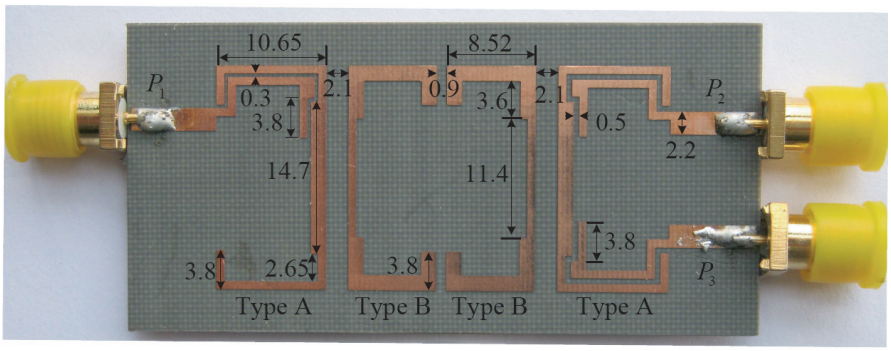

Figure 11. Photograph of the fabricated filtering balun (balun II) and its physical dimensions, all are in mm.

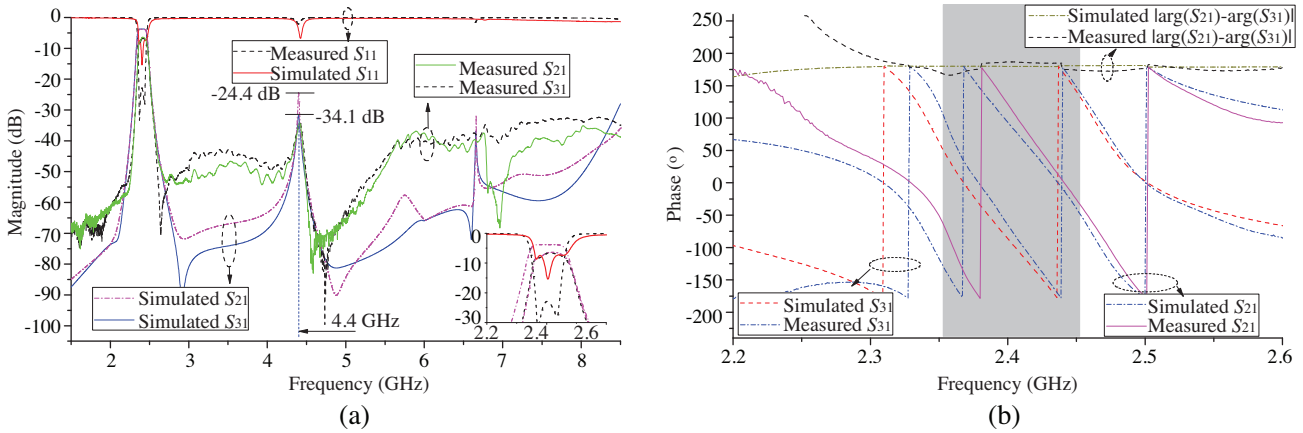

Figure 12. (a) S parameters, (b) phase and phase difference of the two output ports of filtering balun (balun II).

less than 10° is observed. As shown in Fig. 12, except for the central frequency and magnitude unbalance level of the two output ports, a large discrepancy exists between the measured and simulated results. It may be due to the unexpected tolerance of fabrication and implementation. However, as a experimental confirmation, the measured results verify the effectiveness of the proposed filtering balun and the design procedure. The total size is $21.6 \times 44.0\,\text{mm}^2$, about $0.25\lambda_g \times 0.51\lambda_g$, where λ_g is the guided wavelength of the 50-Ω microstrip line at 2.4 GHz.

5. CONCLUSION

A bandpass filter with wide stopband and its corresponding filtering balun are presented in this paper. They are constructed by four SIRs which are designed to have different high-order resonant frequencies. By this way, the spurious responses are effectively suppressed. A more general design procedure is introduced in detail, which starts with the conventional design of a bandpass filter. By introducing two identical coupling output ports for the output resonator at its two symmetric positions with out-of-phase voltages, out-of-phase output signals are obtained. Two filters with different external coupling structures and their corresponding filtering baluns are designed as examples. They have different stopband performances because of different external coupling styles. It is shown that better stopband performance is observed when utilizing microstrip coupling lines other other than tapped line as the external coupling structure. The filtering balun with coupling line as the external coupling structure is fabricated and measured. Although a large discrepancy between the simulated and measured results exists, the presented filtering balun is effectively verified experimentally.

ACKNOWLEDGMENT

This work was supported by the Natural Science Foundation of Jiangxi Province of China (Grant No. 20151BAB207014).

REFERENCES

1. Lin, S., J. Wang, G. Zhang, and J. Hong, "Design of microstrip tri-mode balun bandpass filter with high selectivity," *Electron. Lett.*, Vol. 51, No. 13, 998–999, 2015.
2. Nam, H., T.-S. Yun, and J.-C. Lee, "A broadband microstrip Marchand balun with vertical coupling structure," *Microw. Opt. Technol. Lett.*, Vol. 49, No. 4, 752–755, 2007.
3. Park, M.-J. and B. Lee, "Stubbed branch line balun," *IEEE Microw. Wireless Compon. Lett.*, Vol. 17, No. 3, 169–171, 2007.

4. Li, J. L., S. W. Qu, and Q. Xue, "Miniaturised branch-line balun with bandwidth enhancement," *Electron. Lett.*, Vol. 43, No. 17, 931–932, 2007.
5. Pu, X. Y., X. Y. Zhou, S. Y. Zheng, and Y. L. Long, "Wide band balun filter using open/shorted coupled line sections," *Microw. Opt. Technol. Lett.*, Vol. 57, No. 5, 1099–1101, 2015.
6. Jung, E.-Y. and H.-Y. Hwang, "A balun-BPF using a dual mode ring resonator," *IEEE Microw. Wireless Compon. Lett.*, Vol. 17, No. 9, 652–654, 2007.
7. Gao, S. S. and S. Sun, "Compact dual-mode balun bandpass filter with improved upper stopband performance," *Electron. Lett.*, Vol. 47, No. 23, 1281–1283, 2011.
8. Kang, S. J. and H. Y. Hwang, "Ring-balun-bandpass filter with harmonic suppression," *IET Microw. Antennas Propag.*, Vol. 4, No. 11, 1847–1854, 2010.
9. Cheong, P., T.-S. Lv, W.-W. Choi, and K.-W. Tam, "A compact microstrip square-loop dual-mode balun-bandpass filter with simultaneous spurious response suppression and differential performance improvement," *IEEE Microw. Wireless Compon. Lett.*, Vol. 21, No. 2, 77–79, 2011.
10. Sun, S. and W. Menzel, "Novel dual-mode balun bandpass filters using single cross-slotted patch resonator," *IEEE Microw. Wireless Compon. Lett.*, Vol. 21, No. 8, 415–417, 2011.
11. Hui, J. N., W. J. Feng, and W. Q. Che, "Balun bandpass filter based on multilayer substrate integrated waveguide power divider," *Electron. Lett.*, Vol. 48, No. 10, 571–573, 2012.
12. Jiang, W., L. Zhou, A. M. Gao, W. Shen, W. Y. Yin, and J.-F. Mao, "Compact dual-mode dual-band balun filter using double-sided parallel-strip line," *Electron. Lett.*, Vol. 48, No. 21, 1351–1352, 2012.
13. Hao, Z.-C., W.-Q. Ding, and X.-P. Huo, "A wideband high selectivity filtering balun," *Microw. Opt. Technol. Lett.*, Vol. 57, No. 5, 1107–1110, 2015.
14. Leong, Y. C., K. S. Ang, and C. H. Lee, "A derivation of a class of 3-port baluns from symmetrical 4-port networks," *IEEE MTT-S Int. Microwave Symp. Digest*, 1165-1168, 2002.
15. Wu, C.-H., C.-Y. Wang, and C. H. Chen, "Balanced-to-unbalanced bandpass filters and the antenna application," *IEEE Trans. Micro. Theory Tech.*, Vol. 56, No. 11, 2474–2482, 2008.
16. Yang, T., M. Tamura, and T. Itoh, "Compact hybrid resonator with series and shunt resonances used in miniaturized filters and balun filters," *IEEE Trans. Micro. Theory Tech.*, Vol. 58, No. 2, 390–402, 2010.
17. Huang, G.-S. and C. H. Chen, "Dual-band balun bandpass filter with hybrid structure," *IEEE Microw. Wireless Compon. Lett.*, Vol. 21, No. 7, 356–358, 2011.
18. Feng, W.-J. and W. Che, "Wideband balun bandpass filter based on a differential circuit," *IEEE MTT-S Int. Microwave Symp. Digest*, 1–3, 2012.
19. He, Y. and L. Sun, "Dual-band balun bandpass filter using coupled lines with shunt open-ended stubs," *Microw. Opt. Technol. Lett.*, Vol. 56, No. 10, 2358–2360, 2014.
20. Yeung, L. K. and K.-L. Wu, "A dual-band coupled-line balun filter," *IEEE Trans. Micro. Theory Tech.*, Vol. 55, No. 11, 2406–2411, 2007.
21. Armando, F.-P., A. Lujambio, J. Martel, F. Medina, F. Mesa, and R. R. Boix, "Simple and compact balanced bandpass filters based on magnetically coupled resonators," *IEEE Trans. Micro. Theory Tech.*, Vol. 63, No. 6, 1843–1853, 2015.
22. Wu, C.-H., C.-H. Wang, and C. H. Chen, "Balanced coupled-resonator bandpass filters using multisection resonators for common-mode suppression and stopband extension," *IEEE Trans. Micro. Theory Tech.*, Vol. 55, No. 8, 1756–1763, 2007.
23. Wu, L.-S., Y.-X. Guo, J.-F. Mao, and W.-Y. Yin, "Design of a substrate integrated waveguide balun filter based on three-port coupled-resonator circuit model," *IEEE Microw. Wireless Compon. Lett.*, Vol. 21, No. 5, 252–254, 2011.
24. Hong, J. S. and M. J. Lancaster, *Microstrip Filter for RF/Microwave Applications*, John Wiley & Sons, 2001.